RIS-Empowered Anti-Jamming Integrated Communications and Sensing (AJ-ICS) Systems

Journal:	*IEEE Transactions on Vehicular Technology*
Manuscript ID	VT-2025-00657
Manuscript Type:	Correspondence
Date Submitted by the Author:	05-Feb-2025
Complete List of Authors:	Li, Zheng; Zhengzhou University School of Electrical and Information Engineering Zhu, Zhengyu; Zhengzhou University School of Electrical and Information Engineering; Xidian University State Key Laboratory of Integrated Services Network Chu, Zheng; University of Nottingham Ningbo China Liu, Rang; University of California Irvine Gong, Kexian; Zhengzhou University School of Electrical and Information Engineering Xiao, Pei; University of Surrey Institute for Communications Systems Lee, Inkyu; Korea University School of Electrical Engineering
Keywords:	Communication systems, Jamming

RIS-Empowered Anti-Jamming Integrated Communications and Sensing (AJ-ICS) Systems

Zheng Li, *Student Member, IEEE*, Zhengyu Zhu, *Senior Member, IEEE*, Zheng Chu, *Member, IEEE*, Rang Liu, *Member, IEEE*, Kexian Gong, Pei Xiao, *Senior Member, IEEE*, and Inkyu Lee, *Fellow, IEEE*

***Abstract*—Integrated communications and sensing (ICS) systems in intelligent transportation systems hold significant promise for future 6G networks, where robust anti-jamming capabilities are critically demanded. This paper investigates an anti-jamming framework leveraging reconfigurable intelligent surfaces (RIS) for ICS systems operating in environments with imperfect channel state information (CSI). We propose a joint optimization framework that designs transmit beamforming, receive filters, and RIS phase shifts to simultaneously enhance communication rates and radar signal-to-interference-plus-noise ratio (SINR). The formulated problem is non-convex due to coupled variables, and thus we develop an iterative algorithm combining majorization-minimization (MM) and successive convex approximation (SCA) techniques. The receive filter is optimized using a closed-form minimum variance distortionless response solution, while the transmit beamforming is addressed through semidefinite programming relaxation. For RIS phase shift optimization, we utilize MM and SCA to decompose the problem into manageable convex subproblems. The simulations show that our proposed scheme achieves notable improvements in both the communication rate and radar SINR. The findings of this work provide insights for a design of ICS systems in future intelligent transportation applications, particularly in interference-prone environments.**

***Index Terms*—Anti-Jamming, Integrated Communications and Sensing, Reconfigurable intelligent surface.**

I. Introduction

Transportation systems have been evolving beyond traditional ground networks into three-dimensional spaces, driven by advancements in Intelligent Transportation Systems (ITS) and Urban Air Mobility (UAM) [1]. This transformation requires robust communication and sensing capabilities for secure operations. Integrated Communication and Sensing (ICS) systems address this need by combining communication and sensing functions, offering an efficient solution for both terrestrial and aerial transportation through optimized spectrum use and hardware integration [2]. The fusion of radar sensing and communication functionalities significantly enhances spectral efficiency while reducing system complexity and energy consumption, providing comprehensive solutions for vehicle localization, and obstacle detection. Concurrently, Reconfigurable Intelligent Surfaces (RIS) have emerged as an easily deployable wireless communication enhancement technology, offering new possibilities for smart urban wireless environments [3]. Through active manipulation of electromagnetic wave reflections and scattering, the RIS can substantially improve channel conditions between aerial vehicles, ground infrastructure, and other transportation participants, and increase the system capacity [4]. The synergy of RIS and ICS technologies enhances both vehicular and aerial network communication performance and improves traffic sensing accuracy, paving the way for advanced intelligent transportation networks. Also, it provides significant potential for improving aerial safety, mitigating traffic congestion, and optimizing three-dimensional traffic flow management [5].

In a dynamic ITS environment, unauthorized or non-cooperative devices, such as non-standard vehicular equipment, personal Wi-Fi hotspots, and even malicious jammers, can generate severe interference, significantly degrading ICS system performance. This interference undermines the reliability of vehicle-to-vehicle communications and compromises traffic sensing accuracy, posing risks to road safety and efficiency. However, the RIS technology can enhance the anti-jamming capabilities of ICS systems by actively reshaping the electromagnetic environment. By dynamically adjusting the phase of its reflecting elements, RIS improves the Signal-to-Interference-plus-Noise Ratio (SINR) of the systems without additional power consumption [6]. Moreover, large-scale RIS deployment creates diverse signal propagation paths, increasing spatial diversity and enhancing system robustness against various interference types. Consequently, integrating RIS into ICS systems elevates overall ITS performance and builds more reliable intelligent transportation networks, particularly in urban environments [7]. In a related study [8], a RIS-assisted ICS framework was proposed for intelligent transportation, focusing on the joint optimization of base station (BS) beamforming and RIS phase shifts. The goal was to maximize radar mutual information while adhering to user rate constraints under imperfect angle and channel state information. An innovative approach for enhancing physical-layer security in ICS systems was presented in [9]. By deriving an approximate ergodic achievable secrecy rate, the authors developed an optimization framework that maximizes security while satisfying both communication and sensing requirements. This correspondence presents a RIS-assisted anti-jamming scheme for ICS systems under imperfect channel state information, leveraging the flexible electromagnetic manipulation capabilities of RIS

Z. Li, Z. Zhu, and K. Gong are with the School of Electrical and Information Engineering, Zhengzhou University, Zhengzhou, 450001, China, and Z. Zhu is also with State Key Laboratory of Integrated Services Networks, Xidian University, Xi'an, 710071, China (e-mail: stones_li@outlook.com, zhuzhengyu6@gmail.com, kxgong@zzu.edu.cn).

Z. Chu is with the Department of Electrical and Electronic Engineering, University of Nottingham Ningbo China, Ningbo 315100, China (e-mail: andrew.chuzheng7@gmail.com).

Rang Liu is with the Center for Pervasive Communications and Computing, University of California, Irvine, CA 92697 USA (e-mail: rangl2@uci.edu).

P. Xiao is with the 5GIC & 6GIC, Institute for Communication Systems (ICS), University of Surrey, Guildford GU2 7XH, UK (e-mail: p.xiao@surrey.ac.uk).

I. Lee is with the School of Electrical Engineering, Korea University, Seoul, Korea (e-mail: inkyu@korea.ac.kr).

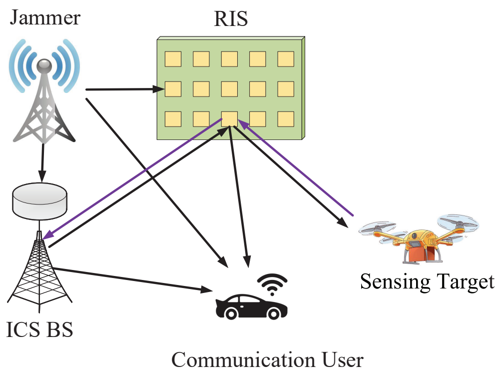

Fig. 1. System model

to enhance both communication and sensing performance. The optimization problem is formulated to jointly design the receive filter, the beamforming strategy, and RIS phase shifts, with the dual objectives of maximizing the communication rate and radar SINR.

II. System Model

The system model under consideration, depicted in Fig. 1, involves an RIS-assisted ICS system operating within an intelligent transportation environment. The setup includes an ICS base station (BS), an RIS, a communication user, a sensing target, and a source of interference. The BS is equipped with a uniform linear array (ULA) comprising N_T transmit antennas and N_R receive antennas. For analytical simplicity, we assume $N_T = N_R = N$. The BS transmits communication signals to the user while performing sensing operations on the target. To enhance both communication and sensing capabilities, an RIS with N_L elements is deployed and managed by a dedicated controller, which can dynamically adjust the phase shifts to optimize the propagation environment. In the context of ITS, various unauthorized or non-cooperative wireless devices may act as interference sources, potentially disrupting both the communication reliability and sensing accuracy of the ICS system. We consider a scenario where perfect channel state information (CSI) is not available. Similar to [10], we model the imperfect channel as

$$\mathbf{h} \triangleq \tilde{\mathbf{h}} + \varsigma \leqslant \left(1 - \sqrt{\psi}\right) \tilde{\mathbf{h}}, \tag{1}$$

where $\tilde{\mathbf{h}}$ is the estimated channel and ς signifies the channel uncertainties with $\|\varsigma\|^2 \leqslant \psi \left\|\tilde{\mathbf{h}}\right\|^2$, with ψ being the error factor.

In the considered ICS system, the BS transmits a signal expressed as

$$\mathbf{x} = \mathbf{w}s, \tag{2}$$

where $\mathbf{w} \in \mathbb{C}^{N\times 1}$ denotes the transmit beamforming vector and s indicates the ICS symbol. The signal received at the communication user can be formulated as

$$y_c = (\mathbf{h}_d + \mathbf{h}_c \mathbf{\Theta} \mathbf{H})\, \mathbf{w}s + \sqrt{P_J}\left(f_{d,c} + \mathbf{h}_c \mathbf{\Theta} \mathbf{f}_{r,c}\right) q + n, \tag{3}$$

where $\mathbf{h}_d \in \mathbb{C}^{1\times N}$ represents the direct channel from the BS to the user, $\mathbf{h}_c \in \mathbb{C}^{1\times N_L}$ denotes the channel between the RIS and the user, $\mathbf{H} \in \mathbb{C}^{N_L\times N}$ corresponds to the channel from the BS to the RIS. $f_{d,c}$ is the channel between the jammer and the user, the $\mathbf{f}_{r,c} \in \mathbb{C}^{1\times N_L}$ represents the channel between the jammer and the RIS, P_J is the transmit power of the jammer and q equals the transmit signal of the jammer with $\mathbb{E}\left\{qq^H\right\} = 1$, and n is the additive white Gaussian noise (AWGN) with variance σ_c^2. The reflection matrix is defined as $\mathbf{\Theta} = \mathrm{diag}\left(\mathbf{v}\right)$, where $\mathbf{v} = [v_1, ..., v_{N_L}]$ is the vector of reflection coefficients, each satisfying the unit modulus constraint $|v_l| = 1, l \in [1, N_L]$. Based on the received signal at the user, the SINR can be expressed as

$$\gamma_c = \frac{\mathbb{E}\left\{\left|(\mathbf{h}_d + \mathbf{h}_c \mathbf{\Theta} \mathbf{H})\, \mathbf{w}s\right|^2\right\}}{P_J \mathbb{E}\left\{\left|\left(f_{d,c} + \mathbf{h}_c \mathbf{\Theta} \mathbf{f}_{r,c}\right) q\right|^2\right\} + \sigma_c^2}. \tag{4}$$

In terms of the sensing operation, we assume that the ICS BS can perfectly handle the cancellation of self-interference. The signal transmission follows a two-stage process. Initially, the transmitted signal propagates to the target through RIS-reflected paths, followed by the target reflection back to the ICS BS. The received echo signal at the BS receive array can be formulated as

$$\tilde{\mathbf{y}}_r = \alpha_0 (\mathbf{H}\mathbf{\Theta}\mathbf{h}_t)^H (\mathbf{h}_t \mathbf{\Theta}\mathbf{H})\, \mathbf{w}s + \sqrt{P_J}\left(\mathbf{f}_{d,s} + \mathbf{f}_{r,s}\mathbf{\Theta}\mathbf{H}\right) q + \mathbf{n}_s, \tag{5}$$

where α_0 denotes the target's radar cross section (RCS), $\mathbf{f}_{d,s} \in \mathbb{C}^{N\times 1}$ represents the channel between the jammer and the BS, $\mathbf{f}_{r,s} \in \mathbb{C}^{N_L\times 1}$ characterizes the channel between the jammer and the RIS, $\mathbf{n}_s$ indicates the AWGN noise with variance σ_r^2 at the BS. Upon signal reception, a complex Gaussian $N \times 1$ complex receive filter $\mathbf{u}$ is applied to process the incoming signals efficiently. After filtering, the processed signal y_r can be expressed as

$$\begin{aligned} y_r &= \alpha_0 \mathbf{u}^H \left(\mathbf{H}\mathbf{\Theta}\mathbf{h}_t\right)^H \left(\mathbf{h}_t\mathbf{\Theta}\mathbf{H}\right) \mathbf{w}s \\ &\quad + \sqrt{P_J}\mathbf{u}^H \left(\mathbf{f}_{d,s} + \mathbf{f}_{r,s}\mathbf{\Theta}\mathbf{H}\right) q + \mathbf{u}^H \mathbf{n}_s. \end{aligned} \tag{6}$$

Thus, the radar SINR for sensing is given as

$$\gamma_r = \frac{\mathbb{E}\left\{\left|\alpha_0 \mathbf{u}^H \left(\mathbf{H}\mathbf{\Theta}\mathbf{h}_t\right)^H \left(\mathbf{h}_t\mathbf{\Theta}\mathbf{H}\right) \mathbf{w}s\right|^2\right\}}{P_J \mathbb{E}\left\{\left|\mathbf{u}^H \left(\mathbf{f}_{d,s} + \mathbf{f}_{r,s}\mathbf{\Theta}\mathbf{H}\right) q\right|^2\right\} + \sigma_r^2 \mathbf{u}^H \mathbf{u}}. \tag{7}$$

This study focuses on enhancing system performance by optimizing the weighted combination of the achievable communication rate and the radar SINR. To achieve this goal, we jointly optimize the receiving filter $\mathbf{u}$, the transmitting beamforming vector $\mathbf{w}$, and the RIS phase shift matrix $\mathbf{\Theta}$. The corresponding optimization problem is formulated as

$$\max_{\mathbf{w},\mathbf{\Theta},\mathbf{u}} \ \rho \log\left(1 + \gamma_c\right) + \left(1 - \rho\right) \gamma_r \tag{8a}$$

$$\text{s.t. } \|\mathbf{w}\|^2 < P_c, \tag{8b}$$

$$|v_l| = 1, l \in [1, N_L], \tag{8c}$$

where (8b) sets the transmit power budget P_c and (8c) enforces unit modulus RIS constraints. The problem (8) is non-convex due to the objective function (8a).

III. Proposed Solution

To address the formulated optimization problem, we develop an efficient iterative algorithm based on an alternating optimization framework. Specifically, the original problem is decomposed into three subproblems: receive filter optimization, transmit beamforming design and RIS phase shift optimization. For the receive filter design, we derive a closed-form solution based on the minimum variance distortionless response (MVDR) principle [11]. Also, the transmit beamforming subproblem is addressed through semidefinite programming relaxation, while the RIS phase shifts are optimized using a combination of majorization-minimization (MM) and successive convex approximation (SCA) techniques.

A. Receive Filter Design

To simplify derivations, we define $\mathbf{H}_t = \left(\mathbf{H}^H\mathbf{\Theta}\mathbf{h}_t^H\right)(\mathbf{h}_t\mathbf{\Theta}\mathbf{H}) \in \mathbb{C}^{N\times N}$ and $\mathbf{h}_J = (\mathbf{f}_{d,s}+\mathbf{f}_{r,s}\mathbf{\Theta}\mathbf{H}) \in \mathbb{C}^{N\times 1}$. For a given transmit beamforming vector $\mathbf{w}$ and RIS phase shift matrix $\mathbf{\Theta}$, the optimal receive filter can be obtained by solving the following optimization problem

$$\max_{\mathbf{u}} \frac{\left|\alpha_0\mathbf{u}^H\mathbf{H}_t\mathbf{w}s\right|^2}{P_J\mathbf{u}^H\mathbf{h}_J\mathbf{h}_J^H\mathbf{u}+\sigma_r^2\mathbf{u}^H\mathbf{u}}, \tag{9}$$

where the maximization problem can be equivalently transformed into an MVDR problem [11] as

$$\begin{aligned} &\min_{\mathbf{u}} \mathbf{u}^H(P_J\mathbf{h}_J\mathbf{h}_J^H+\sigma_r^2\mathbf{I})\mathbf{u} \\ &\text{s.t. } \mathbf{u}^H\mathbf{H}_t\mathbf{w}=1. \end{aligned} \tag{10}$$

Following the MVDR principle, the optimal receive filter can be derived in closed form as

$$\mathbf{u} = \frac{\left(P_J\mathbf{h}_J\mathbf{h}_J^H+\sigma_r^2\mathbf{I}\right)^{-1}\mathbf{H}_t\mathbf{w}}{\mathbf{w}^H{\mathbf{H}_t}^H\left(P_J\mathbf{h}_J\mathbf{h}_J^H+\sigma_r^2\mathbf{I}\right)^{-1}\mathbf{H}_t\mathbf{w}}. \tag{11}$$

B. Transmit Beamforming Design

With the optimal receive filter obtained in (11), we proceed to optimize the transmit beamforming vector $\mathbf{w}$. To facilitate the problem formulation, we define $\mathbf{h}_1 \triangleq \mathbf{h}_d + \mathbf{h}_c\mathbf{\Theta}\mathbf{H}$, $\mathbf{H}_d \triangleq (\mathbf{h}_d+\mathbf{h}_c\mathbf{\Theta}\mathbf{H})^H(\mathbf{h}_d+\mathbf{h}_c\mathbf{\Theta}\mathbf{H})$ and $\mathbf{H}_{tt} \triangleq \mathbf{H}_t\mathbf{H}_t^H$. Then, for fixed RIS phase shifts $\mathbf{\Theta}$, the optimization problem with respect to the transmit beamforming vector $\mathbf{w}$ can be given as

$$\begin{aligned} \max_{\mathbf{w}} \rho\log&\left(1+\frac{|\mathbf{h}_1\mathbf{w}s|^2}{P_J|(f_{d,c}+\mathbf{h}_c\mathbf{\Theta}\mathbf{f}_{r,c})\,q|^2+\sigma_c^2}\right) \\ &+(1-\rho)\frac{\left|\alpha_0\mathbf{u}^H\mathbf{H}_t\mathbf{w}\right|^2}{P_J|\mathbf{u}^H\mathbf{h}_Jq|^2+\sigma_r^2\mathbf{u}^H\mathbf{u}} \end{aligned} \tag{12a}$$

$$\text{s.t. } \|\mathbf{w}\|^2 < P_c. \tag{12b}$$

By defining $\mathbf{W} \triangleq \mathbf{w}\mathbf{w}^H$ and utilizing the semidefinite programming (SDP) technique, problem (12) can be given as

$$\begin{aligned} \max_{\mathbf{W}} \ \rho\log&\left(1+\frac{\mathrm{Tr}\left(\mathbf{H}_d\mathbf{W}\right)}{P_J|(f_{d,c}+\mathbf{h}_c\mathbf{\Theta}\mathbf{f}_{r,c})\,q|^2+\sigma_c^2}\right) \\ &+\frac{(1-\rho)\alpha_0^2\mathbf{u}^H\mathbf{u}\mathrm{Tr}\left(\mathbf{H}_{tt}\mathbf{W}\right)}{P_J|\mathbf{u}^H\mathbf{h}_Jq|^2+\sigma_r^2\mathbf{u}^H\mathbf{u}} \end{aligned} \tag{13a}$$

$$\text{s.t.}\,\mathrm{Tr}\left(\mathbf{W}\right) < P_c, \tag{13b}$$

$$\mathrm{Rank}(\mathbf{W}) = 1. \tag{13c}$$

By removing the non-convex rank-one constraint on the beamforming matrix $\mathbf{W}$ in (13c), the original problem can be relaxed into a convex semidefinite program (SDP). This relaxed formulation enables the application of convex optimization techniques to efficiently compute the optimal beamforming solution. To solve this optimization problem (13), we first compute the SDP solution $\mathbf{W}$ by temporarily relaxing the rank-one constraint. When the obtained solution $\mathbf{W}$ satisfies the rank-one property, the optimal vector solution can be directly extracted through eigenvalue decomposition (EVD). Nevertheless, in cases where the rank of $\mathbf{W}$ exceeds one, we employ Gaussian randomization techniques to transform the higher-rank solution into a feasible rank-one solution [12]. Specifically, we generate M_L independent random vectors $\xi_t \sim \mathcal{CN}(0,\mathbf{W})$ for $t=1,\ldots,M_L$. Each candidate beamforming vector is constructed as $\mathbf{w}_t = \sqrt{P_c}\xi_t/|\xi_t|$ to satisfy the power constraint. Among these M_L candidates, we select the one that yields the highest objective value. This randomization procedure has been shown to provide a good approximate solution with high probability, typically achieving performance close an the upper bound given by the relaxed SDP when M_L is sufficiently large. This randomization approach effectively balances solution feasibility while approximating the optimal objective value of the original problem.

C. Phase shifts Design

After determining the optimal receive filter $\mathbf{u}$ and transmit beamforming vector $\mathbf{w}$, we proceed to optimize the RIS phase shifts. To make the problem more tractable, we utilize the relationship

$$\mathbf{h}_c\mathbf{\Theta}\mathbf{H} = \mathbf{v}\mathrm{diag}\left(\mathbf{h}_c\right)\mathbf{H}, \tag{14}$$

which allows us to reformulate equations (4) and (7) as

$$\begin{aligned} \gamma_c &= \frac{|(\mathbf{h}_d+\mathbf{v}\mathrm{diag}\left(\mathbf{h}_c\right)\mathbf{H})\,\mathbf{w}s|^2}{P_J|(f_{d,c}+\mathbf{v}\mathrm{diag}\left(\mathbf{h}_c\right)\mathbf{f}_{r,c})\,q|^2+\sigma_c^2} \\ &= \frac{\mathbf{v}\mathbf{E}\mathbf{v}^H+\mathbf{v}\mathbf{g}_1+\mathbf{g}_1^H\mathbf{v}^H+\delta_1}{\mathbf{v}\mathbf{F}_1\mathbf{v}^H+\mathbf{v}\mathbf{f}_1+\mathbf{f}_1^H\mathbf{v}^H+\delta_2}, \end{aligned} \tag{15}$$

where $\mathbf{g}_1 = \mathbf{G}\mathbf{W}\mathbf{h}_d^H$, $\mathbf{E} = \mathbf{G}\mathbf{W}\mathbf{G}^H$, $\mathbf{f}_1 = P_J\mathrm{diag}\left(\mathbf{f}_{r,c}\right)\mathbf{f}_{j,c}f_{d,c}$, $\mathbf{F}_1 = P_J\left(\mathrm{diag}\left(\mathbf{f}_{r,c}\right)\mathbf{f}_{j,c}\right)\left(\mathrm{diag}\left(\mathbf{f}_{r,c}\right)\mathbf{f}_{j,c}\right)^H$, $\delta_1 = \mathbf{h}_d^H\mathbf{h}_d$, and $\delta_2 = P_Jf_{d,c}f_{d,c}^H+\sigma_c^2$. Let us define $f_j = \mathbf{u}^H\mathbf{f}_{d,s}$, $\mathbf{f}_{jj} = \mathbf{u}^H\mathbf{H}\mathrm{diag}\left(\mathbf{f}_{r,s}\right)$, $\mathbf{F}_{22} = P_J\mathbf{f}_{jj}\mathbf{f}_{jj}^H$, $\mathbf{f}_2 = P_Jf_j\mathbf{f}_{jj}^H$, and $\delta_3 = P_Jf_jf_j^H+\sigma_r^2\mathbf{u}^H\mathbf{u}$. After some mathematical manipulations, the radar SINR (7) can be simplified in (16), which is presented at the top of this page.

Thus, the problem (8) can be written

$$\begin{aligned} &\max_{\mathbf{v}} \rho\log\left(1+\frac{\mathbf{v}\mathbf{E}\mathbf{v}^H+\mathbf{v}\mathbf{g}_1+\mathbf{g}_1^H\mathbf{v}^H+\delta_1}{\mathbf{v}\mathbf{F}_1\mathbf{v}^H+\mathbf{f}_1\mathbf{v}+\mathbf{v}^H\mathbf{f}_1^H+\delta_2}\right) \\ &\quad+\frac{(1-\rho)\alpha_0^2\mathbf{u}^H\mathbf{G}^H\mathbf{v}^H\mathbf{v}\mathbf{G}\mathbf{W}\left(\mathbf{G}\mathbf{v}^H\mathbf{v}\mathbf{G}^H\right)^H\mathbf{u}}{\mathbf{v}\mathbf{F}_{22}\mathbf{v}^H+\mathbf{v}\mathbf{f}_2+\mathbf{f}_2^H\mathbf{v}^H+\delta_3} \\ &\text{s.t. } |v_l| = 1, l\in[1,N_L]. \end{aligned} \tag{17}$$

To solve this problem, we define $\mathbf{x} \triangleq \mathrm{vec}\left\{\mathbf{v}^{\mathbf{H}}\mathbf{v}\right\} = \mathbf{v}\otimes\mathbf{v}$ and $\mathbf{G}_1 \triangleq (1-\rho)\alpha_0^2\left[\left(\mathbf{G}\mathbf{W}\mathbf{G}^H\right)\otimes\left(\mathbf{G}^H\mathbf{u}\mathbf{u}^H\mathbf{G}\right)\right]$. Then the radar SINR numerator can be written in (18) at the top of the following page by applying the transformation $\mathrm{Tr}\left\{\mathbf{ABCD}\right\} = \mathrm{vec}^H\left\{\mathbf{D}^H\right\}\left(\mathbf{C}^T\otimes\mathbf{A}\right)\mathrm{vec}\left\{\mathbf{B}\right\}$. The (18) holds by applying the transformation $\mathrm{Tr}\left\{\mathbf{ABCD}\right\} = \mathrm{vec}^H\left\{\mathbf{D}^H\right\}\left(\mathbf{C}^T\otimes\mathbf{A}\right)\mathrm{vec}\left\{\mathbf{B}\right\}$. The term $\mathbf{x}^H\mathbf{G}_1\mathbf{x}$ in the objective function is a quartic in terms function of the variable $\mathbf{v}$, rendering the optimization problem intractable. Then, we employ the MM algorithm to construct a tractable surrogate function majorizing the objective. Specifically, by leveraging

$$
\begin{aligned}
\gamma_r &= \frac{\left|\alpha_0 \mathbf{u}^H \left(\mathbf{H}^H \boldsymbol{\Theta} \mathbf{h}_t^H\right)\left(\mathbf{h}_t \boldsymbol{\Theta} \mathbf{H}\right) \mathbf{w} s\right|^2}{P_J \left|\mathbf{u}^H \left(\mathbf{f}_{d,s} + \mathbf{H}\boldsymbol{\Theta}\mathbf{f}_{r,s}\right) q\right|^2 + \sigma_r^2 \mathbf{u}^H \mathbf{u}} = \frac{\left|\alpha_0 \mathbf{u}^H \left(\mathbf{H}^H \mathrm{diag}\left(\mathbf{h}_t^H\right) \mathbf{v}^H\right)\left(\mathbf{v}\mathrm{diag}\left(\mathbf{h}_t\right)\mathbf{H}\right)\mathbf{w}\right|^2}{P_J \left|\left(\mathbf{u}^H \mathbf{f}_{d,s} + \mathbf{u}^H \mathbf{H}\mathrm{diag}\left(\mathbf{f}_{r,s}\right)\mathbf{v}^H\right)\right|^2 + \sigma_r^2 \mathbf{u}^H \mathbf{u}} \\
&= \frac{\alpha_0^2 \mathbf{u}^H \mathbf{G}^H \mathbf{v}^H \mathbf{v} \mathbf{G} \mathbf{W} \left(\mathbf{G}\mathbf{v}^H \mathbf{v}\mathbf{G}\right)^H \mathbf{u}}{P_J \left|\left(f_j + \mathbf{f}_{jj}\mathbf{v}^H\right)\right|^2 + \sigma_r^2 \mathbf{u}^H \mathbf{u}} = \frac{\alpha_0^2 \mathbf{u}^H \mathbf{G}^H \mathbf{v}^H \mathbf{v} \mathbf{G} \mathbf{W} \left(\mathbf{G}\mathbf{v}^H \mathbf{v}\mathbf{G}\right)^H \mathbf{u}}{\mathbf{v}\mathbf{F}_{22}\mathbf{v}^H + \mathbf{v}\mathbf{f}_2 + \mathbf{f}_2^H \mathbf{v}^H + \delta_3},
\end{aligned} \tag{16}
$$

$$
\begin{aligned}
&(1-\rho)\alpha_0^2 \mathbf{u}^H \mathbf{G}^H \mathbf{v}^H \mathbf{v} \mathbf{G} \mathbf{W} \left(\mathbf{G}^H \mathbf{v}^H \mathbf{v} \mathbf{G}\right)^H \mathbf{u} = (1-\rho)\alpha_0^2 \mathrm{Tr}\left\{\mathbf{G}\mathbf{u}\mathbf{u}^H \mathbf{G}^H \mathbf{v}^H \mathbf{v} \mathbf{G} \mathbf{W} \mathbf{G}^H \mathbf{v}^H \mathbf{v}\right\} \\
&= (1-\rho)\alpha_0^2 \mathrm{vec}^H \left\{\mathbf{v}^H \mathbf{v}\right\}\left[\left(\mathbf{G}\mathbf{W}\mathbf{G}^H\right) \otimes \left(\mathbf{G}^H \mathbf{u}\mathbf{u}^H \mathbf{G}\right)\right] \mathrm{vec}\left\{\mathbf{v}^H \mathbf{v}\right\} = \mathbf{x}^H \mathbf{G}_1 \mathbf{x}.
\end{aligned} \tag{18}
$$

the second-order Taylor expansion, we derive an upper bound for $\mathbf{x}^H\mathbf{G}_1\mathbf{x}$ at a given point $\mathbf{x}_s$ i.e. $\mathbf{v}_s$ as

$$
\begin{aligned}
&\mathbf{x}^H \mathbf{G}_1 \mathbf{x} \leqslant \lambda_{\mathbf{G}_1} \mathbf{x}^H \mathbf{x} + 2\Re\left\{\mathbf{x}^H (\mathbf{G}_1 - \lambda_{\mathbf{G}_1} \mathbf{I}_{N_L R^2})\mathbf{x}_s\right\} \\
&+ \mathbf{x}_s^H (\lambda_{\mathbf{G}_1} \mathbf{I}_{N_L{}^2} - \mathbf{G}_1)\mathbf{x}_s.
\end{aligned} \tag{19}
$$

Considering the amplitude constraint imposed on the optimization variable $\mathbf{x}$, it follows

$$
\mathbf{x}^H \mathbf{x} = (\mathbf{v}\mathbf{v}^H) \otimes (\mathbf{v}\mathbf{v}^H) = {N_L}^2. \tag{20}
$$

Denoting $f_N(\mathbf{a})$ as a function which returns an $N \times N$ matrix out of a vector $\mathbf{a}$ of length N^2, we further obtain

$$
\mathbf{x}^H \mathbf{G}_1 \mathbf{x} \leq \Re\left\{\mathbf{x}^H \mathbf{g}_2\right\} + \delta_4 = \Re\left\{\mathbf{v}\mathbf{G}_2\mathbf{v}^H\right\} + \delta_4, \tag{21}
$$

where $\mathbf{g}_2 \triangleq 2(\mathbf{G}_1 - \lambda_{\mathbf{G}_1}\mathbf{I}_{N_L^2})\mathbf{x}_s$, $\delta_4 \triangleq \lambda_{\mathbf{G}_1}{N_L}^2 + \mathbf{x}_s^H(\lambda_{\mathrm{G}_1}\mathbf{I}_{N_L^2} - \mathbf{G}_1)\mathbf{x}_s$, and $\mathbf{G}_2 = f_{N_L}(\mathbf{g}_2)$. Since the term $\Re\left\{\mathbf{v}\mathbf{G}_2\mathbf{v}^H\right\}$ is non-convex, the complex-valued function is transformed into its real-valued equivalent as

$$
\bar{\mathbf{v}} \triangleq [\Re\{\mathbf{v}\} \;\; \Im\{\mathbf{v}\}]^H, \bar{\mathbf{G}}_2 \triangleq \begin{bmatrix} \Re\{\mathbf{G}_2\} & \Im\{\mathbf{G}_2\} \\ \Im\{\mathbf{G}_2\} & -\Re\{\mathbf{G}_2\} \end{bmatrix}. \tag{22}
$$

We subsequently apply the second-order Taylor expansion as

$$
\begin{aligned}
\bar{\mathbf{v}}^T \bar{\mathbf{G}}_2 \bar{\mathbf{v}} &\leqslant \bar{\mathbf{v}}_s^T \bar{\mathbf{G}}_2 \bar{\mathbf{v}}_s + \bar{\mathbf{v}}_s^T \left(\bar{\mathbf{G}}_2 + \bar{\mathbf{G}}_2^T\right)(\bar{\mathbf{v}} - \bar{\mathbf{v}}_s) \\
&+ \frac{\lambda_{\tilde{g}}}{2}(\bar{\mathbf{v}} - \bar{\mathbf{v}}_s)^T (\bar{\mathbf{v}} - \bar{\mathbf{v}}_s) \\
&= \frac{\lambda_{\tilde{g}}}{2}\mathbf{v}\mathbf{v}^H + \Re\left\{\mathbf{v}\tilde{\mathbf{g}}^H\right\} + \delta_5,
\end{aligned} \tag{23}
$$

where $\lambda_{\tilde{g}} = \lambda_{\max}\left(\bar{\mathbf{G}}_2 + \bar{\mathbf{G}}_2^T\right)$, $\tilde{\mathbf{g}} = [\mathbf{I}_{N_L} \; j\mathbf{I}_{N_L}]\left(\bar{\mathbf{G}}_2 + \bar{\mathbf{G}}_2^T - \lambda_{\tilde{g}}\mathbf{I}_{2N_L}\right)\bar{\mathbf{v}}_s$, and $\delta_5 = -\bar{\mathbf{v}}_s^T \bar{\mathbf{G}}_2 \bar{\mathbf{v}}_s + \frac{\lambda_{\tilde{g}}}{2}\bar{\mathbf{v}}_s^T \bar{\mathbf{v}}_s$.

Thus, we have

$$
\mathbf{x}^H \mathbf{G}_1 \mathbf{x} \leqslant \frac{\lambda_{\tilde{g}}}{2}\mathbf{v}\mathbf{v}^H + \Re\left\{\mathbf{v}\tilde{\mathbf{g}}^H\right\} + \delta_4 + \delta_5, \tag{24}
$$

Therefore, the objective function for $\mathbf{v}$ is transformed to

$$
\mathbf{v}\mathbf{G}_3\mathbf{v}^H + \Re\left\{\mathbf{v}\tilde{\mathbf{g}}^H\right\} + \delta_6, \tag{25}
$$

where $\mathbf{G}_3 \triangleq \frac{\lambda_{\tilde{g}}\mathbf{I}_{N_L}}{2}$ and $\delta_6 \triangleq \delta_4 + \delta_5 = \lambda_{\mathbf{G}_1}{N_L}^2 + \mathbf{x}_s^H(\lambda_{\tilde{g}}\mathbf{I}_{N_L{}^2} - \mathbf{G}_1)\mathbf{x}_s - \bar{\mathbf{v}}_s^T\bar{\mathbf{G}}_2\bar{\mathbf{v}}_s + \frac{\lambda_{\tilde{g}}}{2}\bar{\mathbf{v}}_s^T\bar{\mathbf{v}}_s$. Then, denoting $\tilde{\mathbf{v}} \triangleq [\mathbf{v} \; 1]$ and

$$
\mathbf{E}_1 = \begin{bmatrix} \mathbf{E} & \mathbf{g}_1^H \\ \mathbf{g}_1 & \delta_1 \end{bmatrix} \qquad \mathbf{F}_2 = \begin{bmatrix} \mathbf{F}_1 & \mathbf{f}_1^H \\ \mathbf{f}_1 & \delta_2 \end{bmatrix}
$$

$$
\mathbf{F}_2 = \begin{bmatrix} \mathbf{F}_1 & \mathbf{f}_1^H \\ \mathbf{f}_1 & \delta_2 \end{bmatrix} \quad \mathbf{G}_4 = \begin{bmatrix} \mathbf{G}_3 & \tilde{\mathbf{g}}^H \\ \tilde{\mathbf{g}} & \delta_6 \end{bmatrix},
$$

the problem can be written as

$$
\begin{aligned}
&\max_{\tilde{\mathbf{v}}} \rho \log\left(1 + \frac{\tilde{\mathbf{v}}\mathbf{E}_1\tilde{\mathbf{v}}^H}{\tilde{\mathbf{v}}\mathbf{F}_2\tilde{\mathbf{v}}^H}\right) + \frac{(1-\rho)}{2}\frac{\tilde{\mathbf{v}}\mathbf{G}_4\tilde{\mathbf{v}}^H}{\tilde{\mathbf{v}}\mathbf{F}_4\tilde{\mathbf{v}}^H} \\
&\text{s.t.} \; |v_l| = 1, l \in [1, N_L + 1].
\end{aligned} \tag{26}
$$

For the problem (26), we use the SCA technique to linearize as

$$
\begin{aligned}
&\max_{\tilde{\mathbf{v}}} \rho \log\left(1 + \frac{\tilde{\mathbf{v}}_k\mathbf{E}_1\tilde{\mathbf{v}}_k^H}{\tilde{\mathbf{v}}_k\mathbf{F}_2\tilde{\mathbf{v}}_k^H}\right) + \frac{(1-\rho)}{2}\frac{\tilde{\mathbf{v}}_k\mathbf{G}_4\tilde{\mathbf{v}}_k^H}{\tilde{\mathbf{v}}_k\mathbf{F}_4\tilde{\mathbf{v}}_k^H} \\
&\quad + \nabla f(\tilde{\mathbf{v}}_k)(\tilde{\mathbf{v}} - \tilde{\mathbf{v}}_k) \\
&\text{s.t.} \; |v_l| = 1, l \in [1, N_L + 1]
\end{aligned} \tag{27}
$$

where $\nabla f(\tilde{\mathbf{v}}_k) = \nabla f_1(\tilde{\mathbf{v}}_k) + \nabla f_2(\tilde{\mathbf{v}}_k)$, $\nabla f_1(\tilde{\mathbf{v}}_k) = \rho\left(\frac{2\mathbf{E}_1\tilde{\mathbf{v}}_k^H}{\tilde{\mathbf{v}}_k\mathbf{E}_1\tilde{\mathbf{v}}_k^H + \tilde{\mathbf{v}}_k\mathbf{F}_2\tilde{\mathbf{v}}_k^H} - \frac{(\tilde{\mathbf{v}}_k\mathbf{E}_1\tilde{\mathbf{v}}_k^H)\mathbf{F}_2\tilde{\mathbf{v}}_k^H}{(\tilde{\mathbf{v}}_k\mathbf{E}_1\tilde{\mathbf{v}}_k^H + \tilde{\mathbf{v}}_k\mathbf{F}_2\tilde{\mathbf{v}}_k^H)(\tilde{\mathbf{v}}_k\mathbf{F}_2\tilde{\mathbf{v}}_k^H)}\right)$, and $\nabla f_2(\tilde{\mathbf{v}}_k) = \frac{(1-\rho)}{2}\left(\frac{\mathbf{G}_4\tilde{\mathbf{v}}_k^H}{\tilde{\mathbf{v}}_k\mathbf{F}_4\tilde{\mathbf{v}}_k^H} - \frac{(\tilde{\mathbf{v}}_k\mathbf{G}_4\tilde{\mathbf{v}}_k^H)\mathbf{F}_4\tilde{\mathbf{v}}_k^H}{(\tilde{\mathbf{v}}_k\mathbf{F}_4\tilde{\mathbf{v}}_k^H)^2}\right)$. Then, problem (27) becomes a convex problem and can be efficiently solved by the CVX toolbox.

D. Computational Complexity Analysis

The complexity of optimizing the receive filter using the MVDR principle is $\mathcal{O}\left(N^3\right)$, which mainly comes from the matrix inversion operation. Second, for the transmit beamforming optimization using SDP relaxation, the computational complexity equals $\mathcal{O}\left(N^{3.5}\right)$, where the dominant factor is solving the semidefinite programming problem. Finally, the RIS phase shift optimization, which involves both MM and SCA iterations, has the highest complexity of $\mathcal{O}\left(I_m I_s {N_L}^{3.5}\right)$, where I_m and I_s represent the number of MM and SCA iterations respectively.

IV. SIMULATION RESULTS

In this section, we introduce the simulation setup for our system. The coordinates for the BS, RIS, user, jammer, and target are (0m, 0m), (6m, 8m), (10m, 8m), (0m, 100m), and (8m, 6m), respectively. The channels between the BS-RIS, BS-user, and RIS-user are modeled as $\mathbf{h}_d = L_d\left(\sqrt{\frac{K_0}{K_0+1}}\mathbf{h}_d^{\mathrm{LoS}} + \sqrt{\frac{1}{K_0+1}}\mathbf{h}_d^{\mathrm{NLoS}}\right)$, $\mathbf{h}_c = L_c\left(\sqrt{\frac{K_0}{K_0+1}}\mathbf{h}_c^{\mathrm{LoS}} + \sqrt{\frac{1}{K_0+1}}\mathbf{h}_c^{\mathrm{NLoS}}\right)$ and $\mathbf{H} = L_H\left(\sqrt{\frac{K_0}{K_0+1}}\mathbf{H}^{\mathrm{LoS}} + \sqrt{\frac{1}{K_0+1}}\mathbf{H}^{\mathrm{NLoS}}\right)$, respectively, where K_0 is set as 6 dB and $L_i = C_0(d_i/d_0)^{-\alpha_i}, i \in [d, c, H]$. Here, d_i and α_i are the distance and the path loss exponent with C_0 = -30 dB, respectively. The path loss exponent of BS-RIS, RIS-user, and BS-User equal $\alpha_H = 2.5$, $\alpha_c = 2.5$ and $\alpha_d = 3$. The LoS components for these links are calculated based on the angle of arrival and the distance between the corresponding nodes. The NLoS components are modeled using a Rayleigh fading distribution. The Los link dominates in sensing, thus the channel $\mathbf{h}_t$ is established as

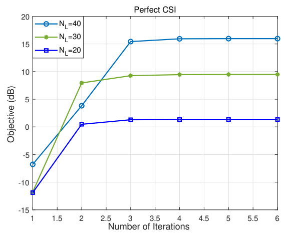

Fig. 2. Objective versus the number of iterations

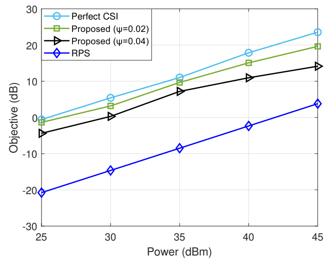

Fig. 3. Objective versus power

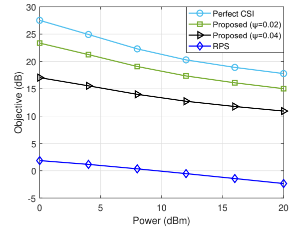

Fig. 4. Objective versus jamming power

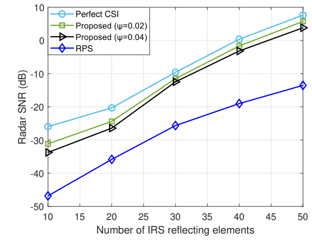

Fig. 5. Radar SINR versus the number of RIS reflecting element

a LoS channel between the RIS and the target. The channels between the Jammer-ICS BS, the Jammer-RIS, and the jammer-user are similarly established to incorporate both the distance-dependent path loss and the Rayleigh fading. Therefore, we have $\mathbf{f}_{d,s} = L_{d,s}\left(\sqrt{\frac{K_0}{K_0+1}}\mathbf{f}_{d,s}^{\mathrm{LoS}} + \sqrt{\frac{1}{K_0+1}}\mathbf{f}_{d,s}^{\mathrm{NLoS}}\right)$, $\mathbf{f}_{r,s} = L_{d,s}\left(\sqrt{\frac{K_0}{K_0+1}}\mathbf{f}_{r,s}^{\mathrm{LoS}} + \sqrt{\frac{1}{K_0+1}}\mathbf{f}_{r,s}^{\mathrm{NLoS}}\right)$, and $f_{d,c} = L_{d,s}\left(\sqrt{\frac{K_0}{K_0+1}}f_{d,c}^{\mathrm{LoS}} + \sqrt{\frac{1}{K_0+1}}f_{d,c}^{\mathrm{NLoS}}\right)$. The path loss exponent of the Jammer-ICS BS, the Jammer-RIS, and the jammer-user are set as $\alpha_{d,s} = 2.5$, $\alpha_{r,s} = 2.2$, and $\alpha_{d,c} = 2$. The transmit power is $P = 40$ dBm, the power of the jammer equals P_J = 20dBm, the noise power is set to $\sigma_c = \sigma_r = -100$ dBm, the RCS is fixed to 1 with $\rho = 0.5$ and $\psi = 0.02$. The proposed scheme is benchmarked against two baseline methods: Perfect CSI scheme with ideal channel knowledge at both ends, and Random Phase Shift (RPS) scheme where RIS elements operate with uniformly distributed random phases.

The simulation results in Fig. 2 show the results of the perfect CSI case. We see that all settings of N_L, the objective value can quickly converge after a few iterations.

Fig. 3 illustrates the performance with respect to the transmit power. We can see that the proposed scheme achieves the performance quite close to the ideal perfect CSI case. Also, our scheme outperforms RPS.

Fig. 4 demonstrates the effect of jamming power on the objective value. Also, it is clear that the proposed scheme performs better than conventional schemes. As the jamming power increases, the objective value experiences a decline for all schemes.

Fig. 5 exhibits the radar performance in terms of RIS reflecting elements. With more RIS elements, the system can focus on the transmitted signal more effectively toward the desired target, and obtain better CSI.

V. Conclusion

In this work, we introduced a novel approach to improve the performance of ICS systems in intelligent transportation environments by leveraging RIS. A joint optimization framework was developed to design the transmit beamforming, receive filter, and RIS phase shifts, effectively tackling the nonconvex optimization problem using MM and SCA techniques. Extensive simulation results demonstrate that our proposed method outperforms existing benchmark schemes, achieving significant enhancements in both communication rates and radar SINR under various system configurations. We conclude that the proposed scheme exhibits strong robustness in jamming-prone scenarios.

References

[1] A. P. Cohen, S. A. Shaheen, and E. M. Farrar, "Urban air mobility: History, ecosystem, market potential, and challenges," *IEEE Trans. Intell. Transp. Syst.*, vol. 22, no. 9, pp. 6074–6087, Sep. 2021.

[2] Z. Li, Z. Zhu, Z. Chu, Y. Guan, D. Mi, F. Liu, and L.-L. Yang, "Intelligent reflective surface assisted integrated sensing and wireless power transfer," *IEEE Trans. Intell. Transp. Syst.*, vol. 25, no. 10, pp. 15122–15127, Oct. 2024.

[3] Z. Zhu, Z. Li, Z. Chu, Q. Wu, J. Liang, Y. Xiao, P. Liu, and I. Lee, "Intelligent reflecting surface-assisted wireless powered heterogeneous networks," *IEEE Trans. Wirel. Commun.*, vol. 22, no. 12, pp. 9881–9892, Dec. 2023.

[4] R. Liu, M. Li, H. Luo, Q. Liu, and A. L. Swindlehurst, "Integrated sensing and communication with reconfigurable intelligent surfaces: Opportunities, applications, and future directions," *IEEE Wirel. Commun.*, vol. 30, no. 1, pp. 50–57, Feb. 2023.

[5] Z. Chen, P. Chen, Z. Guo, Y. Zhang, and X. Wang, "A RIS-based vehicle DOA estimation method with integrated sensing and communication system," *IEEE Trans. Intell. Transp. Syst.*, vol. 25, no. 6, pp. 5554–5566, Jun. 2024.

[6] R. Liu, M. Li, Q. Liu, and A. Lee Swindlehurst, "SNR/CRB-constrained joint beamforming and reflection designs for RIS-ISAC systems," *IEEE Trans. Wirel. Commun.*, vol. 23, no. 7, pp. 7456–7470, Jul. 2024.

[7] M. Rihan, A. Zappone, S. Buzzi, G. Fodor, and M. Debbah, "Passive versus active reconfigurable intelligent surfaces for integrated sensing and communication: Challenges and opportunities," *IEEE Netw.*, vol. 38, no. 3, pp. 218–226, May 2024.

[8] M. Luan, B. Wang, Z. Chang, T. Hämäläinen, and F. Hu, "Robust beamforming design for RIS-aided integrated sensing and communication system," *IEEE Trans. Intell. Transp. Syst.*, vol. 24, no. 6, pp. 6227–6243, Jun. 2023.

[9] Z. Xing, R. Wang, and X. Yuan, "Reconfigurable intelligent surface aided physical-layer security enhancement in integrated sensing and communication systems," *IEEE Trans. Veh. Tech.*, vol. 73, no. 4, pp. 5179–5196, Apr. 2024.

[10] H.-V. Tran and G. Kaddoum, "Robust design of AC computing-enabled receiver architecture for SWIPT networks," *IEEE Wireless Commun. Lett.*, vol. 8, no. 3, pp. 801–804, Jun. 2019.

[11] R. Liu, M. Li, Q. Liu, and A. Lee Swindlehurst, "Joint transmit waveform and receive filter design for dual-functional radar-communication systems," in *Proc. IEEE ICC, Seoul, South Korea*, May 2022, pp. 5116-5121.

[12] Z.-Q. Luo, W.-K. Ma, A. M.-C. So, Y. Ye, and S. Zhang, "Semidefinite relaxation of quadratic optimization problems," *IEEE Signal Proce. Mag.*, vol. 27, no. 3, pp. 20–34, May 2010.